Year: 2013

Metal artefact reduction from dental hardware in carotid CT angiography using iterative reconstructions

Morsbach, Fabian ; Wurnig, Moritz ; Kunz, Daniel M ; Krauss, Andreas ; Schmidt, Bernhard ; Kollias, Spyros S ; Alkadhi, Hatem

Abstract: PURPOSE: To determine the value of a metal artefact reduction (MAR) algorithm with iterative reconstructions for dental hardware in carotid CT angiography. METHODS: Twenty-four patients (six of which were women; mean age 70 ± 12 years) with dental hardware undergoing carotid CT angiography were included. Datasets were reconstructed with filtered back projection (FBP) and using a MAR algorithm employing normalisation and an iterative frequency-split (IFS) approach. Three blinded, independent readers measured CT attenuation values and evaluated image quality and degrees of artefacts using axial images, multi-planar reformations (MPRs) and maximal intensity projections (MIP) of the carotid arteries. RESULTS: CT attenuation values of the internal carotid artery on images with metal artefacts were significantly higher in FBP (324 ± 104HU) datasets compared with those reconstructed with IFS (278 ± 114HU; $P < 0.001$) and with FBP on images without metal artefacts (293 ± 106HU; $P = 0.006$). Quality of IFS images was rated significantly higher on axial, MPR and MIP images ($P < 0.05$, each), and readers found significantly less artefacts impairing the diagnostic confidence of the internal carotid artery ($P < 0.05$, each). CONCLUSION: The MAR algorithm with the IFS approach allowed for a significant reduction of artefacts from dental hardware in carotid CT angiography, hereby increasing image quality and improving the accuracy of CT attenuation measurements. KEY POINTS: • CT angiography of the neck has proven value for evaluating carotid disease • Neck CT angiography images are often degraded by artefacts from dental implants • A metal artefact reduction algorithm with iterative reconstruction reduces artefacts significantly • Visualisation of the internal carotid artery is improved.

COMPUTED TOMOGRAPHY

Metal artefact reduction from dental hardware in carotid CT angiography using iterative reconstructions

**Fabian Morsbach · Moritz Wurnig · Daniel M. Kunz ·
Andreas Krauss · Bernhard Schmidt · Spyros S. Kollias ·
Hatem Alkadhi**

Abstract

Purpose To determine the value of a metal artefact reduction (MAR) algorithm with iterative reconstructions for dental hardware in carotid CT angiography.

Methods Twenty-four patients (six of which were women; mean age 70 ± 12 years) with dental hardware undergoing carotid CT angiography were included. Datasets were reconstructed with filtered back projection (FBP) and using a MAR algorithm employing normalisation and an iterative frequency-split (IFS) approach. Three blinded, independent readers measured CT attenuation values and evaluated image quality and degrees of artefacts using axial images, multi-planar reformations (MPRs) and maximal intensity projections (MIP) of the carotid arteries.

Results CT attenuation values of the internal carotid artery on images with metal artefacts were significantly higher in FBP (324 ± 104HU) datasets compared with those reconstructed with IFS (278 ± 114HU; $P<0.001$) and with FBP on images without metal artefacts (293 ± 106HU; $P=0.006$). Quality of IFS images was rated significantly higher on axial, MPR and MIP images ($P<0.05$, each), and readers found significantly less artefacts impairing the diagnostic confidence of the internal carotid artery ($P<0.05$, each).

Conclusion The MAR algorithm with the IFS approach allowed for a significant reduction of artefacts from dental hardware in carotid CT angiography, hereby increasing image quality and improving the accuracy of CT attenuation measurements.

Key points
- *CT angiography of the neck has proven value for evaluating carotid disease*
- *Neck CT angiography images are often degraded by artefacts from dental implants*
- *A metal artefact reduction algorithm with iterative reconstruction reduces artefacts significantly*
- *Visualisation of the internal carotid artery is improved*

Keywords Metal artefact reduction · Computed tomography angiography · Dental implants · Internal carotid artery · Carotid angiography

Abbreviations

MAR	Metal artefact reduction
IFS	Iterative frequency split
MPR	Multiplanar reformation
MIP	Maximum intensity projection
FBP	Filtered back projection
NMAR	Normalised metal artefact reduction

F. Morsbach · M. Wurnig · D. M. Kunz · H. Alkadhi (✉)
Institute of Diagnostic and Interventional Radiology,
University Hospital Zurich, Raemistrasse 100,
8091 Zurich, Switzerland
e-mail: hatem.alkadhi@usz.ch

A. Krauss · B. Schmidt
Siemens Healthcare, Imaging & Therapy Systems Division,
Forchheim, Germany

S. S. Kollias
Department of Neuroradiology, University Hospital Zurich,
Zurich, Switzerland

Introduction

Computed tomography (CT) angiography has become one of the most commonly used modalities to evaluate vascular structures. Due to the development of fast and high-resolution multi-detector CT equipment, CT angiography has replaced invasive catheter angiography for most diagnostic indications.

CT angiography of the neck has proven value for the evaluation of arterio-occlusive disease, acute cranio-cervical trauma and dissection [1, 2]. Furthermore, it is currently used routinely in the evaluation of patients with suspicion of stroke and transient ischaemic attacks [3–5].

The image quality of carotid CT angiography relies upon optimal intraluminal opacification of the carotid arteries, and depends on good timing of the contrast media bolus and a good spatial resolution [6–9]. Often, however, the quality of carotid CT angiography images is impaired by metal artefacts arising from dental hardware. This is caused by the dense metal objects causing streak artefacts in CT images through photon starvation and beam hardening [10]. In fact, recent studies reported non-diagnostic image quality of carotid CT angiography studies ranging between 4.7 % [11] and 28 % [6] caused by metal artefacts from dental hardware. In addition to a reduced image quality, metal artefacts have shown to impair the post-processing of carotid CT angiography images (such as bone removal) considerably [12].

Many attempts have been undertaken for developing metal artefact reduction (MAR) algorithms in CT. Most MAR algorithms employ an inpainting method, which discards all image information polluted by metal artefacts [13, 14]. This approach, however, results in loss of data and therefore potentially important clinical information. Other methods include either reconstruction techniques demanding considerable computational power [15–17] or require dual-energy CT protocols [18–20]. Recently introduced MAR algorithms employ new approaches preserving information with a frequency split approach [21] or normalisation [22] of the images to reduce the amount of newly introduced artefacts reported when using an inpainted MAR algorithm [13, 14]. It has been previously shown how normalisation can improve image quality and reduce artefacts arising from dental hardware in head and neck CT [22].

In the present work, we use a novel MAR algorithm, which combines normalisation and frequency split in an iterative reconstruction process for improving MAR in multiple iterations. This algorithm extends on a previously reported iterative frequency-split algorithm by including three-dimensional (3D) geometry of the CT data [23]. Thus, the purpose of the study was to determine the value of this iterative frequency-split (IFS) algorithm for MAR of dental hardware in patients undergoing carotid CT angiography.

Material and methods

Patient population

In the study period between August and October 2012, a total of 78 consecutive patients underwent carotid CT angiography

in our department for various indications, including follow-up after vascular surgery. From this population, 24 (31 %) patients (18 men, mean age 68 ± 13 years; 6 women, mean age 75 ± 11 years) exhibited artefacts from dental metal hardware in their CT studies and thus were included in the present study.

The study had institutional review board and local ethics committee approval. Written informed consent was waived since all CT studies were clinically indicated, and no CT examination was performed merely for the purpose of this study.

CT imaging

All CT data was acquired with a 128-section dual-source CT machine (SOMATOM Definition Flash, Siemens Healthcare, Forchheim, Germany). Image acquisition was performed in a caudo-cranial direction during mid-inspiration. CT angiography was performed with the following parameters: slice acquisition $2\times0.6\times128$ by means of a z-flying focal spot, gantry rotation 0.5 s, tube voltage of 100 kV, reference tube current-time product 100 mAs with automated, attenuation-based tube current modulation (CAREDose4D; Siemens).

Patients received 80 ml contrast medium (Iopromidum, Ultravist 370, 370 mg iodine/ml; Bayer Schering Pharma, Berlin, Germany) at a flow rate of 5 ml/s. Contrast media was injected over an antecubital vein using a dual-head power injector (Stellant; Medrad, Inianola, USA). CT data acquisition was initiated with bolus tracking via a region of interest (ROI) in the ascending aorta, using a signal attenuation threshold of 120 HU and with a minimum delay of 4 s.

Raw data from carotid CT angiography in these 24 patients were transferred using an external hard drive (Western Digital, Lake Forest, CA, USA) to an offline workstation for further reconstructions.

Iterative metal artefact reduction algorithm

The IFS algorithm for MAR utilises a previously published normalised metal artefact reduction (NMAR) algorithm, which employs linear interpolation with the addition of normalisation and denormalisation of the raw data [24]. At first, prior-images from the raw data are reconstructed using filtered back projection (FBP) and the image is classified into air, soft tissue and bone using HU thresholds. Then pixels identified as air are set to $-1,000$ HU and soft tissue to 0 HU; bone and metal remain unaltered. From these images, a sinogram is calculated using forward projection and normalised with the original raw data sonogram, by division of the prior sinogram pixelwise [24]. Pixels with metal traces in the normalised sinogram are replaced through linear interpolation. Then the sonogram is denormalised and FBP is applied to reconstruct the corrected images. The algorithm replaces the values in the

metal trace of the original raw data; forward projection and FBP operations are therefore based on the original 3D acquisition geometry, which is an extension of the recently published iterative frequency split approach [23].

The NMAR approach relies heavily on correct tissue classification in the reconstructed prior-images. By using already corrected data for the NMAR the classification and thus the image quality can be improved. In an iterative approach, the data for the NMAR is consecutively improved and recalculated. For dental hardware, the algorithm uses EIGHT iterations and a threshold for metal segmentation of 3,000 HU. Additionally, a previously described frequency-split approach [21] is used in image calculation to preserve high frequencies of the original image. This procedure results in less blurring of the image, which can be commonly observed in linear interpolation images [14].

Images were reconstructed with a smooth tissue convolution kernel (B30f) and a field-of-view ranging from 250 to 300 mm, adjusted individually in each patient. After reconstruction, all images were transferred to an external workstation (Multi-Modality Workplace; Siemens Healthcare, Forchheim, Germany).

Image analysis—quantitative

To assess MAR quantitatively, two independent readers (R1 with 4 years of experience and R2 with 3 years of experience in imaging) placed an ROI (average size 0.11 cm^2) in that part of the C1 segment of the ICA [25] which was affected most by streak artefacts on axial images reconstructed with FBP. An ROI of the same size was then placed in the corresponding image at the same level but reconstructed with the IFS algorithm, and the CT attenuation (HU) values in the two datasets were noted.

Additionally, the CT attenuation in the ICA at the level of the carotid bulb, being not affected by metal artefacts, was measured by both readers in the FBP images.

Image analysis—qualitative

Qualitative image analysis was performed by two independent readers (R1 and R3, the latter with 3 years of experience in imaging), blinded to the reconstruction algorithm, on axial source images, as well as on sagittal multi-planar reformations (MPR) of the internal carotid artery (ICA). Semi-quantitative Likert scales were used for the assessment of the C1-segment of the ICA in regard to the overall image quality (score 1 = bad, no diagnosis possible, score 2 = poor, diagnostic confidence substantially reduced; score 3 = moderate, but sufficient for diagnosis; score 4 = good; score 5 =

excellent), as previously shown [8]. The degree of artefact was also assessed using a scoring system (score 1 = complete absence of imaging artefacts; 2 = minor artefacts not interfering with diagnostic decision making; 3 = major artefacts hindering diagnostic decision making) [11]. Both readers graded image quality on axial source images as well as on sagittal MPR.

Additionally, overall image quality of sagittal thin-slab maximum intensity projection (MIP) images (5 mm) of the left and right ICA was qualitatively assessed separately and independently by R1 and R2 using the same score mentioned above.

Statistical analysis

Variables were expressed as mean ± standard deviation. HU values were tested for normality using the Kolmogorov-Smirnoff test.

Inter-reader agreement was assessed using the intraclass correlation coefficient [26].

Student's t-test for paired samples was used to compare CT attenuation in the ICA. The following pairs were formed: FBP reconstructed images affected with metal artefacts compared with IFS reconstructed images at the same level, FBP with metal artefacts compared with FBP without metal artefacts measured at the level of the carotid bulb, IFS at the level of metal artefacts compared to FBP without metal artefacts. Qualitative evaluation of the images was compared with Wilcoxon signed-rank test.

Statistical analysis was performed using commercially available software (IBM SPSS Statistics, version 20, release 20.0.0, Chicago, IL, USA). Significance was inferred at a P value of <0.05. To correct for multiple comparisons of CT attenuation, Bonferroni correction was applied and the significance level was adjusted accordingly to $P<0.017$.

Results

Image data could be reconstructed from the raw data of all 24 patients using the IFS algorithm without problems and with only little user interaction required. Reconstruction time on the offline computer was on average 85 min.

Image analysis—quantitative

Inter-reader agreement for CT attenuation values in all datasets and locations was high (ICC=0.914, $P<0.001$), so the mean CT attenuation from both readers was taken for further analysis.
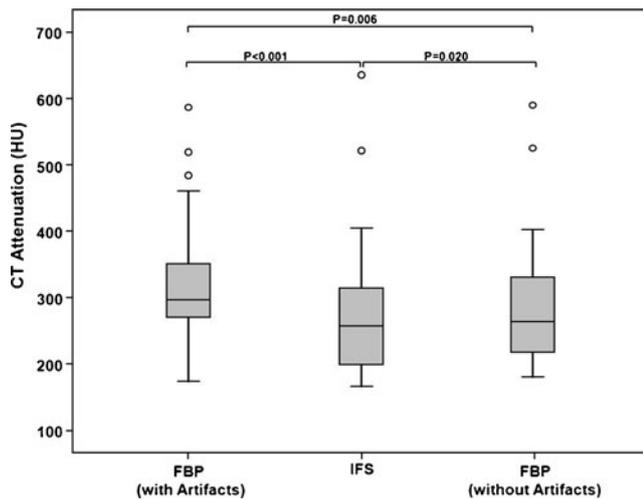
Fig. 1 CT attenuation values in the ICA. Measurements were performed in images reconstructed with filtered-back projection (*FBP*) at a level with highest amounts of artefacts from dental hardware and using the same slice position in images reconstructed with the iterative frequency split (*IFS*) approach. CT attenuation was additionally measured on a slice more caudally at the level of the carotid bulb without metal artefacts. Note the significantly ($P<0.001$) higher CT attenuation in FBP images with artefacts compared with IFS images and FBP images without artefacts, and the comparable CT attenuation values between FBP images without artefacts and IFS images at the level of artefacts

CT attenuation in the ICA measured in FBP images at the level of metal artefacts (324 ± 104 HU) was significantly ($P<0.001$) higher compared with CT attenuation on IFS images (278 ± 114 HU) and also significantly ($P=0.006$) higher compared with CT attenuation on FBP images without metal artefacts measured on the level of the carotid bulb (293 ± 106 HU). In contrast, there were no significant differences in CT attenuation values in the ICA between IFS images at the level of artefacts and FBP images at the level without artefacts ($P=0.020$) (Fig. 1).

Qualitative image evaluation—axial source images

Inter-reader agreement for qualitative image evaluation was high between R1 and R3 for overall image quality (ICC= 0.722, $P<0.001$) and for artefact degree (ICC=0.842, $P<0.001$).

R1 evaluated overall image quality on the axial source images as significantly ($P=0.005$) better for IFS reconstructed images, compared with FBP (2.9 vs 2.4). R1 also found significantly ($P=0.021$) less artefacts impairing diagnostic confidence for IFS compared with FBP (2.3 vs 2.6) (Table 1).

R3 rated overall image quality of IFS on the axial source images better compared with FBP (2.9 vs 2.8); however, without reaching statistical significance ($P=0.317$). Additionally, R3 found significantly ($P=0.001$) less artefacts influencing diagnostic confidence for IFS compared to FBP (2.1 vs 2.5).

Typical imaging examples of patients with various degrees of metal artefacts from dental hardware are shown in Figs. 2 and 3.

Qualitative image evaluation—sagittal multiplanar reformations

Image quality on sagittal MPR was rated significantly ($P=0.021$) better by R1 for IFS compared with FBP (3.1 vs 2.7). Additionally IFS resulted in significantly ($P=0.034$) less artefacts impairing diagnostic confidence when compared with FBP on sagittal MPR (2.2 vs 2.5) (Table 1).

R3 evaluated overall image quality significantly ($P=0.020$) higher for IFS on sagittal MPR compared with FBP on sagittal MPR (3.6 vs 3.2). Artefacts resulting in reduced diagnostic confidence were rated as significantly ($P=0.005$) less on sagittal MPR for IFS compared with FBP (2.0 vs 2.3).
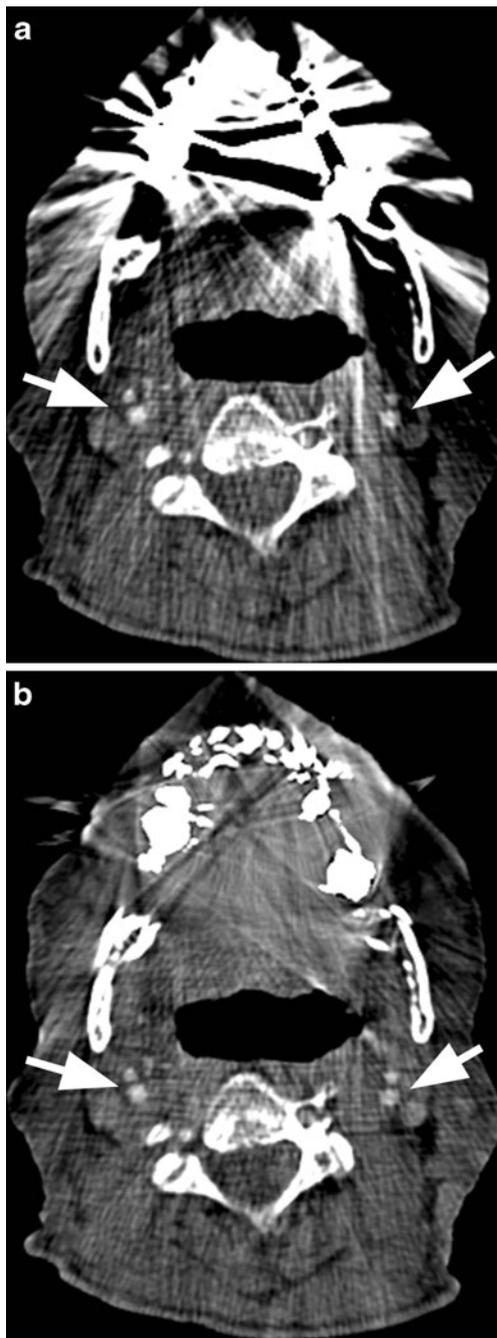
Table 1 Qualitative image evaluation

FBP filtered back projection, *IFS* iterative frequency-split metal artefact reduction

Overall image quality: 1 = bad, no diagnosis possible, 2 = poor, diagnostic confidence substantially reduced, 3 = moderate, but sufficient for diagnosis artefacts, 4 = good, 5 = excellent
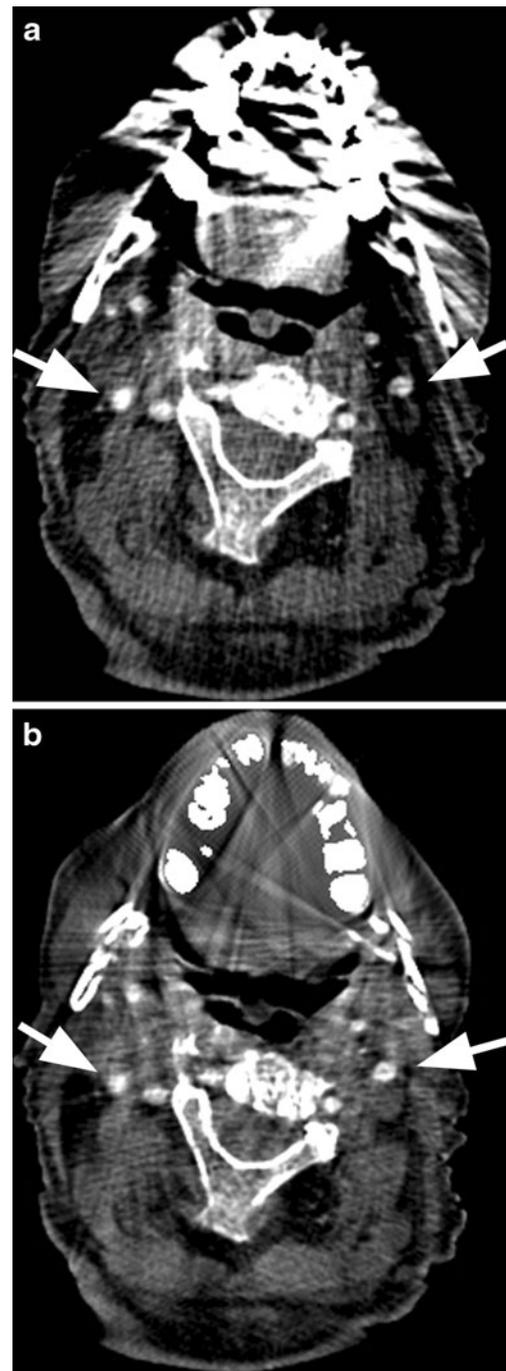
Artefact degree: 3 = major imaging artefacts, 2 = minor imaging artefacts, 1 = complete absence of imaging

			FBP	IFS	*P* value
Reader 1					
	Axial source images	Overall image quality	2.4	2.9	0.005
		Artefact degree	2.6	2.3	0.021
	Multiplanar reformation	Overall image quality	2.7	3.1	0.021
		Artefact degree	2.5	2.2	0.034
	Maximum intensity projection	Overall image quality	2.3	2.7	0.004
Reader 3					
	Axial source images	Overall image quality	2.8	2.9	0.317
		Artefact degree	2.5	2.1	0.001
	Multiplanar Reformation	Overall image quality	3.2	3.6	0.020
		Artefact degree	2.3	2	0.005
Reader 2					
	Maximum intensity projection	Overall image quality	2.3	2.7	0.001

Fig. 2 Axial source images of a 70-year-old-male patient (*arrows* indicating the ICA). Evaluation of the ICA is heavily compromised on images reconstructed with FBP (**a**) due to metal artefacts from dental hardware. Depiction of the ICA is considerably improved on images reconstructed with the IFS algorithm (**b**)

Fig. 3 Axial source images of an 83-year-old male patient with several metal implants reconstructed with FBP (**a**) and IFS (**b**) (*arrows* indicating the ICA). Note streak artefacts impairing image quality of the ICA in FBP. Image quality and depiction of the ICA are considerably improved with IFS

Qualitative image evaluation——sagittal thin-slab maximum intensity projection

A total of 48 ICAs on sagittal MIP images were evaluated, with sagittal MIP images made from reconstructions with both IFS and FBP. Inter-reader agreement between R1 and

R3 for image quality of sagittal MIP images was high (ICC=0.963, *P*<0.001).

R1 found a significantly (*P*=0.004) higher image quality for sagittal MIP images reconstructed from the IFS images compared with FBP-based sagittal MIPs (2.7 vs 2.3).

Similarly, R2 rated image quality of sagittal MIP images from IFS datasets as significantly (*P*=0.001) better than sagittal MIPs from FBP images (2.7 vs 2.3) (Figs. 4 and 5) Table 1.

Discussion

Artefacts arising from metal hardware such as endoprostheses and dental hardware often render CT images non-diagnostic, and potentially crucial lesions could be unrecognised. Image quality of carotid CT angiography is known to be impaired by artefacts arising from dental hardware, as reported in various previous studies in up to 28 % of studies [6, 11]. In our population, we found dental hardware in 31 % of patients impacting on the image quality of carotid CT angiography to various degrees.

Fig. 4 Thin MIP (5-mm) images reconstructed with FBP (**a**) and IFS (**b**) of a 76-year-old female patient with dental hardware. The streak artefacts (*arrow*) are considerably reduced in the images reconstructed with the IFS algorithm
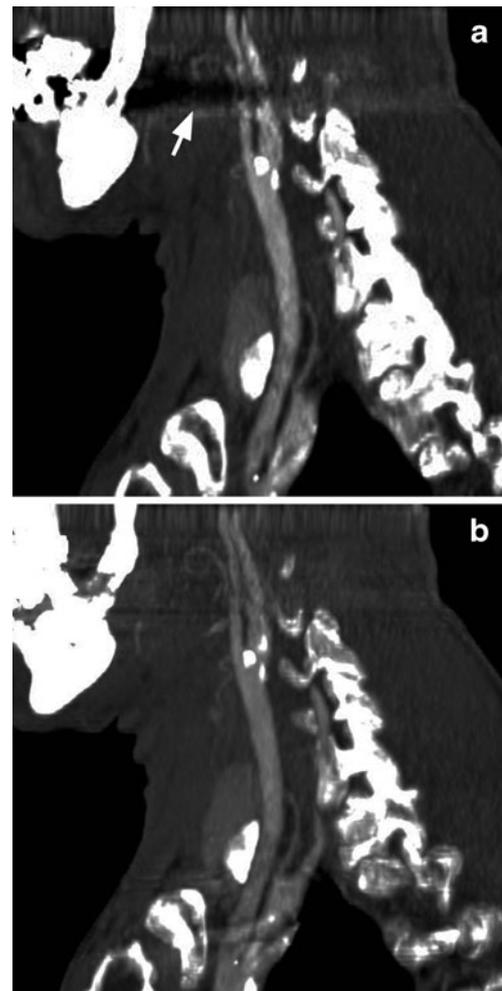
Fig. 5 Thin MIP (5-mm) images reconstructed with FBP (**a**) and IFS (**b**) of a 70-year-old male patient with dental hardware. Artefacts (*arrow*) obscuring the ICA in FBP images are considerably reduced with IFS

Carotid CT angiography is the first-line imaging modality in trauma patients with suspicion of vascular trauma [1, 2], for the evaluation of stenosis with similar accuracy compared with digital subtraction angiography [3, 4], and for the work-up of extracranial vessels in the evaluation of acute stroke [5]. For an accurate evaluation of the ICA, however, it is mandatory to depict the artery with good image quality in its entire length. In addition, CT attenuation measurements should be reliable, as correct assessment of HU values has an effect on window settings for stenosis evaluation [9].

There are some approaches for reducing artefacts from dental hardware in carotid CT angiography. One of the simplest method is tilting the head so that metal causing artefacts is not in the beamline [27]. However, with dental hardware this approach just relocates (but not removes) artefacts to more cranial structures, such as the intracranial arteries. Moreover, in trauma patients, tilting the head is

often contraindicated, or simply not feasible due to neck fixation devices or patient mal-compliance.

Magnetic resonance (MR) angiography of the neck has been shown to be a valuable alternative to CT angiography [28], with dental hardware being rarely a relevant source of artefacts [29]. Thus, MR angiography can be considered an option when there is known excessive dental hardware presumably resulting in non-diagnostic images in CT. However, the extent of dental hardware often is not known prior to imaging, and MR angiography may not be feasible in trauma patients.

There have been multiple approaches to reduce metal artefacts for CT with inpainting methods [13, 14], which is a fast method but is associated with a loss of information. Additionally, iterative reconstruction techniques [15–17] have been previously introduced, but had the drawback of being computationally demanding with up to 50 iterations [17]. Dual-energy protocols with reconstruction of monoenergetic images allow for MAR in titanium-based endoprostheses [18, 19], but require dedicated CT equipment and protocols. Moreover, artefacts from dental hardware usually are too severe to be compensated by monoenergetic reconstructions for dual-energy CT.

Use of iterative reconstructions for reducing noise and for improving image quality has shown value in head and neck CT, having the potential to lower radiation dose for patients [30–32]. The algorithm employed in this study represents a further development including iterative reconstructions into algorithms for metal artefact reduction. Hereby, we use an MAR algorithm based on normalisation [24] and frequency-split [21] combined in an iterative reconstruction approach. The IFS method has the advantage of preserving information normally lost in inpainted methods [21] and is associated with reasonable reconstruction times, which allows its application in clinical routine. In our study the preserved information also translated into more accurate measurement of CT attenuation. Furthermore, this technique does not require specific CT technology and dedicated protocols. We could show that use of the IFS algorithm results in an improved image quality for carotid CT angiography as well as in more stable CT attenuation values of carotid arteries across images with and without metal artefacts. In FBP reconstructed images the HU values were increased due to streak artefacts caused by photon starvation [10]. In contrast, CT attenuation values measured in the ICA at the level of artefacts in the datasets reconstructed with the IFS algorithm were significantly lower, being similar to the values in the ICA in slices not affected by artefacts.

Some study limitations have to be addressed. Firstly, we included a relatively small patient group with different amounts of dental hardware. Secondly, blinding readers to the reconstruction algorithm is not completely possible, as an experienced radiologist might recognise the images reconstructed with the IFS algorithm by their distinctive image impression. Thirdly, we evaluated only the ICA in regard to image quality and CT attenuation, but did not evaluate adjacent cervical soft tissues. Fourthly, we can only state preliminary reconstruction times since the prototype implementation of the reconstruction algorithm is not yet optimised for computation time. Fifthly, we did not compare IFS to any other MAR algorithms or iterative reconstruction methods compared with FBP. Sixthly, we did not evaluate intra-reader reliability, but we showed good inter-reader agreement. Finally, we did not compare carotid CT angiography images reconstructed with the IFS algorithm with the reference standard modality catheter angiography for defining the degree of vessel stenosis, as our patient collective was not referred for stenotic carotid arteries, but for various indications.

Our study indicates that the IFS algorithm employing iterative reconstructions allows for a considerable reduction of metal artefacts arising from dental hardware, along with an increased image quality for evaluation of the ICA in carotid CT angiography studies.

References

1. Utter GH, Hollingworth W, Hallam DK, Jarvik JG, Jurkovich GJ (2006) Sixteen-slice CT angiography in patients with suspected blunt carotid and vertebral artery injuries. J Am Coll Surg 203:838–848

2. Delgado Almandoz JE, Romero JM, Pomerantz SR, Lev MH (2010) Computed tomography angiography of the carotid and cerebral circulation. Radiol Clin North Am 48:265–281, vii–viii

3. Josephson SA, Bryant SO, Mak HK, Johnston SC, Dillon WP, Smith WS (2004) Evaluation of carotid stenosis using CT angiography in the initial evaluation of stroke and TIA. Neurology 63:457–460

4. Koelemay MJ, Nederkoorn PJ, Reitsma JB, Majoie CB (2004) Systematic review of computed tomographic angiography for assessment of carotid artery disease. Stroke 35:2306–2312

5. Latchaw RE, Alberts MJ, Lev MH et al (2009) Recommendations for imaging of acute ischemic stroke: a scientific statement from the American Heart Association. Stroke 40:3646–3678

6. Kim JJ, Dillon WP, Glastonbury CM, Provenzale JM, Wintermark M (2010) Sixty-four-section multidetector CT angiography of carotid arteries: a systematic analysis of image quality and artifacts. AJNR Am J Neuroradiol 31:91–99

7. Ramgren B, Bjorkman-Burtscher IM, Holtas S, Siemund R (2012) CT angiography of intracranial arterial vessels: impact of tube voltage and contrast media concentration on image quality. Acta Radiol 53:929–934

8. Kuroda Y, Hosoya T, Oda A et al (2011) Inverse-direction scanning improves the image quality of whole carotid CT angiography with 64-MDCT. Eur J Radiol 80:749–754

9. Saba L, Mallarin G (2009) Window settings for the study of calcified carotid plaques with multidetector CT angiography. AJNR Am J Neuroradiol 30:1445–1450

Eur Radiol (2013) 23:2687–2694

10. Barrett JF, Keat N (2004) Artifacts in CT: recognition and avoidance. Radiographics 24:1679–1691

11. Borisch I, Boehme T, Butz B, Hamer OW, Feuerbach S, Zorger N (2007) Screening for carotid injury in trauma patients: image quality of 16-detector-row computed tomography angiography. Acta Radiol 48:798–805

12. Lell MM, Hinkmann F, Nkenke E et al (2010) Dual energy CTA of the supraaortic arteries: technical improvements with a novel dual source CT system. Eur J Radiol 76:e6–e12

13. Watzke O, Kalender WA (2004) A pragmatic approach to metal artifact reduction in CT: merging of metal artifact reduced images. Eur Radiol 14:849–856

14. Kalender WA, Hebel R, Ebersberger J (1987) Reduction of CT artifacts caused by metallic implants. Radiology 164:576–577

15. Boas FE, Fleischmann D (2011) Evaluation of two iterative techniques for reducing metal artifacts in computed tomography. Radiology 259:894–902

16. De Man B, Nuyts J, Dupont P, Marchal G, Suetens P (2001) An iterative maximum-likelihood polychromatic algorithm for CT. IEEE Trans Med Imaging 20:999–1008

17. Dong J, Kondo A, Abe K, Hayakawa Y (2011) Successive iterative restoration applied to streak artifact reduction in X-ray CT image of dento-alveolar region. Int J Comput Assist Radiol Surg 6:635–640

18. Bamberg F, Dierks A, Nikolaou K, Reiser MF, Becker CR, Johnson TR (2011) Metal artifact reduction by dual energy computed tomography using monoenergetic extrapolation. Eur Radiol 21:1424–142

19. Guggenberger R, Winklhofer S, Osterhoff G et al (2012) Metallic artefact reduction with monoenergetic dual-energy CT: systematic ex vivo evaluation of posterior spinal fusion implants from various vendors and different spine levels. Eur Radiol 22:2357–2364

20. Stolzmann P, Winklhofer S, Schwendener N, Alkadhi H, Thali MJ, Ruder TD (2013) Monoenergetic computed tomography reconstructions reduce beam hardening artifacts from dental restorations. Forensic Sci Med Pathol. doi:10.1007/s12024-013-9420-z

21. Meyer E, Raupach R, Lell M, Schmidt B, Kachelriess M (2012) Frequency split metal artifact reduction (FSMAR) in computed tomography. Med Phys 39:1904–1916

22. Lell MM, Meyer E, Kuefner MA et al (2012) Normalized metal artifact reduction in head and neck computed tomography. Invest Radiol 47:415–421

23. Morsbach F, Bickelhaupt S, Wanner GA, Krauss A, Schmidt B, Alkadhi H (2013) Reduction of metal artifacts from hip prostheses on CT images of the pelvis: value of iterative reconstructions. Radiology. doi:10.1148/radiol.13122089

24. Meyer E, Raupach R, Lell M, Schmidt B, Kachelriess M (2010) Normalized metal artifact reduction (NMAR) in computed tomography. Med Phys 37:5482–5493

25. Bouthillier A, van Loveren HR, Keller JT (1996) Segments of the internal carotid artery: a new classification. Neurosurgery 38:425–432, discussion 432–423

26. Shrout PE, Fleiss JL (1979) Intraclass correlations: uses in assessing rater reliability. Psychol Bull 86:420–428

27. Brown JH, Lustrin ES, Lev MH, Ogilvy CS, Taveras JM (1999) Reduction of aneurysm clip artifacts on CT angiograms: a technical note. AJNR Am J Neuroradiol 20:694–696

28. Vertinsky AT, Schwartz NE, Fischbein NJ, Rosenberg J, Albers GW, Zaharchuk G (2008) Comparison of multidetector CT angiography and MR imaging of cervical artery dissection. AJNR Am J Neuroradiol 29:1753–1760

29. Klinke T, Daboul A, Maron J et al (2012) Artifacts in magnetic resonance imaging and computed tomography caused by dental materials. PLoS One 7:e31766

30. Rapalino O, Kamalian S, Payabvash S et al (2012) Cranial CT with adaptive statistical iterative reconstruction: improved image quality with concomitant radiation dose reduction. AJNR Am J Neuroradiol 33:609–615

31. Kilic K, Erbas G, Guryildirim M, Arac M, Ilgit E, Coskun B (2011) Lowering the dose in head CT using adaptive statistical iterative reconstruction. AJNR Am J Neuroradiol 32:1578–1582

32. Niu YT, Mehta D, Zhang ZR et al (2012) Radiation dose reduction in temporal bone CT with iterative reconstruction technique. AJNR Am J Neuroradiol 33:1020–1026